Mission Configurable Modular Craft Concept Study

Estudio conceptual de un buque modular configurable por misión

Brant R. Savander,[a]
Armin Troesch[b]

Abstract

This work illustrates how modern high speed craft design tools may be effectively used to evaluate innovative concepts for which empirical data may be limited. The example presented here was motivated by the US Navy's interest in a finding a replacement for, or complement to, the USN Special Operations Forces' Mark V high speed craft. Given the conflicting demands of restricted size and weight imposed by air transportability and broad mission requirements, a modular, multi-hull configuration is proposed and studied. The boat parameter space that influences calm water performance, sea keeping accelerations, and structural loads is explored. A proposed trimaran concept shows how intelligent placement of outer, or wing hulls can, in principle, mitigate shock loads and lower resistance, but with the cost of increased structural complexity and potentially a heavier craft.

Key words: Planing, high-speed craft, multi-hulls, seakeeping

Resumen

Este trabajo muestra cómo las herramientas modernas de diseño de buques de alta velocidad pueden ser usadas para evaluar conceptos innovadores para los que los datos empíricos pueden ser limitados. El ejemplo presentado fue motivado por el interés de la Marina de los EE.UU. en reemplazar o complementar el buque de alta velocidad Mark V. Dados los requerimientos contradictorios de tamaño y peso reducido impuestos para poder ser transportados por aire frente a la capacidad de realizar un amplio rango de misiones, se propone y analiza una configuración modular multicasco. Se realiza la exploración del espacio de diseño de las variables que influencian el desempeño en aguas tranquilas, el comportamiento en el mar y las cargas estructurales. El diseño conceptual tipo trimarán muestra como la disposición adecuada de los cascos externos puede reducir las cargas de impacto y la resistencia del buque a cambio de un aumento en la complejidad estructural y potencialmente el peso de la embarcación.

Palabras claves: Cascos de planeo, embarcaciones de alta velocidad, multicascos, comportamiento en el mar.

[a] Maritime Research Associates,
e-mail: savander@mresearch.us

[b] Department of Naval Architecture and Marine Engineering
University of Michigan

Introduction & Background

A concept design study is documented herein for an air transportable vessel that is to be utilized by special operations forces. Further, the design will allow the vessel to be readily reconfigured to meet the demands of a broad range of mission requirements. Modularity of both the hull and systems components are assessed to support the needs for reconfiguration and air transportability.

Several configurations of mono-hull and multi-hull systems were developed through a high level concept design study, allowing foundation and technical bases to be established for a more detailed preliminary design, Gale (2003), at a later stage. The high level concept design work scope includes preliminary geometry and weight definitions, steady hydrodynamic performance assessment, seakeeping analysis, and structural analysis. Each of the concept designs are documented with emphasis given to air transportability and range of potential mission configurations.

Two central design themes emerged in the process of completing this study. The first design theme was a more conservative approach which focused on redesign of a monohull, similar to the current Mark V, that allowed for air-transportability in a C17 aircraft. This concept is not included in the subsequent sections of this paper.

The second design theme is much less conservative and exhibits significant technical risk. The risk is offset by the potential for increased performance and capabilities that may be desirable for implementation of the SeaPower 21 capstone concept, Clark (2002), through the underlying pillars of Sea Shield, Sea Strike, and Sea Basing. This design approach utilizes modularity to integrate several vessels, many similar to craft in the current SOF (Special Operation Forces) fleet, into one high speed platform. The platform in assembled form is based upon a trimaran concept with a 80 ft centerhull and two 40 ft wing units. The wing units can also be referred to as side hulls. RHIB and CRRC units can be included in the aft bay of the 80 ft centerhull. Additionally, the aft deck area of the wing units could store PWC sized craft. The wing units are detachable and are envisioned to have both manned and unmanned modes of operation.

The trimaran design emphasizes the use of modularity technology to allow a variety of craft, similar to current Mark V, HSAC, RHIB, CRRC, and PWC, which are all capable of independent operations to be assembled into one common high speed vessel. This common vessel relies on the combination and integration of high speed multi-hull and modularity technology with potential unmanned surface vehicle capability. The multi-hull concept is discussed in detail in the section Trimaran Concept Development.

Analysis Methodology

The multi-hull MCMCC concepts were developed through a high level concept design stage. These concepts have coupled high speed and modularity attributes. As a result, emphasis was placed on determining the acceleration loading while operating in a seaway. The acceleration response of the vessel was predicted using the low aspect ratio theory approach defined by Zarnick (1978), Zarnick (1979), and Akers, et al. (1999). Each planing hull form was initially designed, in an iterative manner, based upon steady hydrodynamic performance following Savander, et al. (2002).

The multi-hull concept was first developed at the preliminary level as defined by performance and mission requirements. This information provided the basis for the hull form geometry definition which was defined using steady planing hull hydrodynamic analysis. At the conclusion of the steady hydrodynamic analysis, the hull form was analyzed in a seaway. The loading defined in the seaway calculations were used as input into the preliminary structural design and analysis. The structural computations included local beam element modeling and rules based analysis following the American Bureau of Shipping rules.

Preliminary Concept Design Methodology

The concept design stage is used in this work to establish the feasibility of several different

competing vessel types and configurations to meet the objectives of a Mission Configurable Modular Combatant Craft, MCMCC. Specifically, the MCMCC is to be used by Special Operation Forces (SOF) for a range of potential missions.

The SOF also require that all vessel types considered in this study be air-transportable. The array of potential air transport options are defined in the Table 1 with the two most common options, the C17 and C130, depicted Figure 1. The underlying theme of the entire study was to explore the concept of "modularity" and how modularity could achieve two general objectives.

Table 1. Air Transport options

Air Transport Options				
	C5	**C17**	**C141**	**C130**
Length	121 ft.	85 ft. 2 in.	93 ft. 3 in.	40 ft. 4 in.
Width	19 ft.	18 ft.	10 ft. 3 in.	10 ft.
Height	13.5 ft.	12 ft. 4 in. fwd of wing. 13 ft. 6 in. aft of wing.	9 ft. 1 in.	9 ft.
Payload	216,000 lbs.	170,900 lbs.	94,508 lbs	45,000 lbs

Fig. 1. Most viable air transport options for transformable craft.

C17

C130

C5

C141

The first objective was to determine the feasibility of a vessel that could be,

- disassembled into modules or sub-assemblies;
- packaged for air transport;
- air transported to a remote forward insertion point;
- complete the specified mission;
- return to a remote forward extraction point;
- disassembled and re-packaged for air transport at extraction point; and,
- air transported back to a home base.

The second objective was to utilize the modularity attribute to allow the vessel to be configured to perform a wider array of missions than would be practical for a non-modular vessel. The concept of

modularity produced two general design themes, as also discussed in the Introduction and Background section.

The approach documented in this paper was to develop a multi-hull vessel that exhibited increased performance when compared to a mono-hull vessel like the Mark V. The goal was to increase the speed, range, and seakeeping performance by adding one or more hulls to the monohull configuration. Initially, both a catamaran and a trimaran concept were contemplated. The trimaran concept was selected for concept design development over the catamaran due to several advantages in air transportability and modes of operation.

Steady Hydrodynamic Analysis Methodology

A hydrodynamic model which is based upon slender body theory, as presented in Savander, et al. (2002), was used to compute the steady hydrodynamic performance of the hull forms discussed in this report. This analysis methodology was derived as an extension of the works of Tulin (1957), Vorus (1996), and Savander (1997). An overview of the method is contained below.

The formulation utilizes the traditional ideal flow assumptions that ignore the effects of viscosity and compressibility. The three-dimensional field equation written in terms of the perturbation potential is reduced to a series of two dimensional problems by assuming sufficiently small longitudinal variation in hull geometry to allow for application of slenderness assumptions. As the hull form passes through a fixed transverse frame of reference, as shown in Figure 2, each transverse section of the hull appears to be falling through the free surface. The cross-sectional impact velocity, $V(t)$, can be defined by specification of the hull trim angle, keel curvature, and hull forward velocity. The longitudinal coordinate is related to the sectional time variable by the relation $x = Ut$.

Two distinct flow phases, "chines-dry" (CD) and "chines-wet" (CW), are encountered and are shown in Fig. 2. The chines-dry term refers to the impact phase which is characterized by the free surface and body contour intersection remaining inboard of the chine. In reference to Fig.2, a hull cross-section is shown moving downward through the water surface with velocity, $V(t)$. The zero pressure point, $z_c(x)$, and jet head position, $z_b(x)$, proceed to move outboard with increasing keel depth, $y_{wl}(x)$. The chines-wet, or post impact immersion, phase is encountered when $z_c(x) = z_{cb}(x)$. The jet head position can continue to move outward with continued immersion depth during the CW phase. The CW phase continues until the transom is encountered at which point the calculation is terminated.

The boundary value problem that is solved includes satisfaction of a coupled system defined by a

Fig. 2. Planing surface passing through a transverse plane located in an earth fixed coordinate system

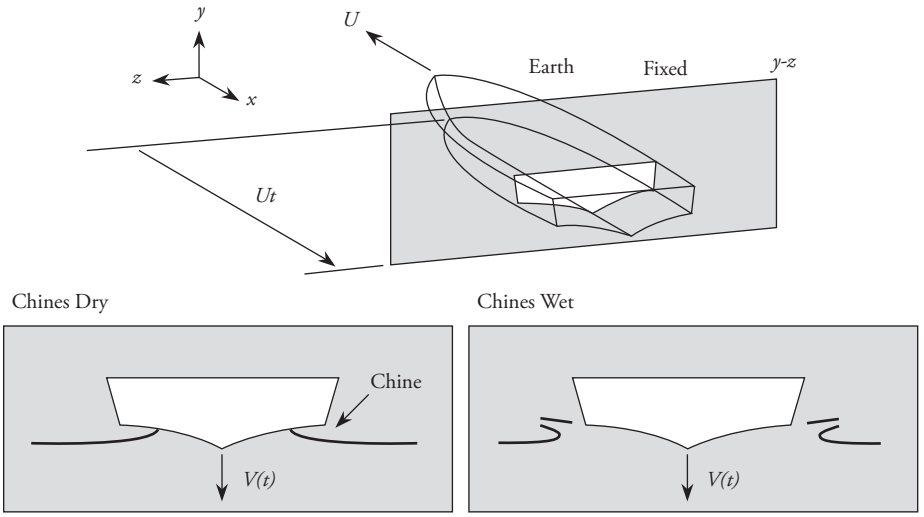

Fig. 3. Hydrodynamic definitions utilized in the cross-flow plane. (Refer to Fig. 2.)

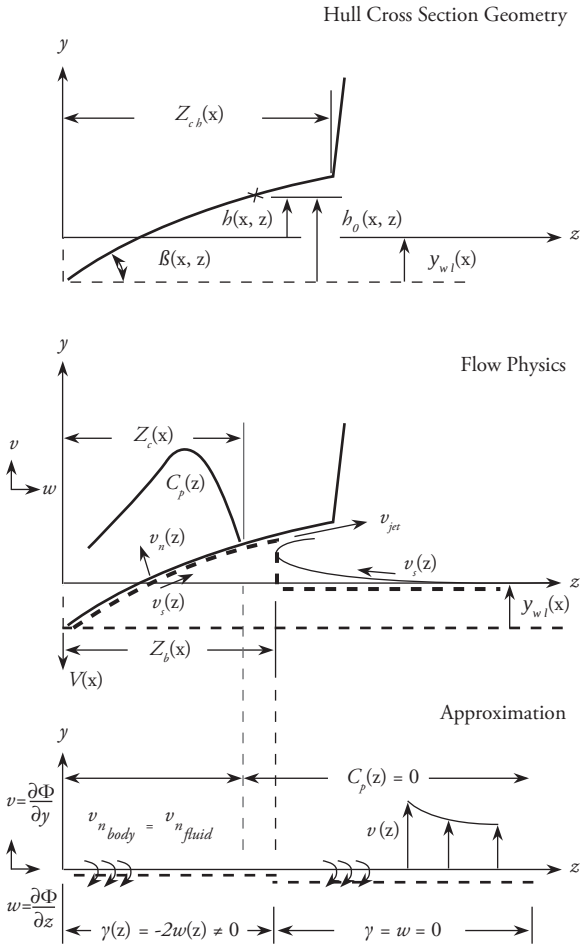

kinematic, dynamic, and displacement continuity condition. The kinematic boundary condition requires the following condition,

$$\vec{\mathbf{v}}_{fluid} \cdot \hat{\mathbf{n}} = \vec{\mathbf{v}}_{body} \cdot \hat{\mathbf{n}} . \tag{1}$$

be satisfied. The condition defined in Eq. (1) requires that the normal component of the hull surface velocity equal the fluid normal velocity on the hull contour. This condition is satisfied through use of a vortex lattice system and application of the Biot-Savart Law. The integral equation that results for the unknown vortex sheet strength, *γ(x,z)*, is,

$$\frac{1}{2}\gamma(x,\zeta)\tan(x,\zeta) + \frac{1}{2\pi}\int_{z_o=-b(x)}^{b(x)} \frac{\gamma(x;\zeta_o)}{\zeta_o - z}\, d\zeta_o \tag{2}$$

$$= -\tan(\alpha(x) - F(x,\zeta)$$

$\zeta \in$ [0,1], where, $b(x) = z_b(x) / z_c(x)$, and $\zeta = z / z_c(x)$

The local keel trim angle is defined by, *α(x)*. The inclusion of the general term, *F(x,ζ)*, in Eq. (2) was first presented by Savander (1997). This function could also represent any function that varies in *(x,ζ)*. Therefore, *F(x,ζ)* can be written in the following form,

$$F(x,\zeta) = \frac{\partial}{\partial x} h_o(x,z) + \sum_{i=1}^{M} H_i(x,\zeta) \tag{3}$$

Solution of (2) following Savander, et al (2002) yields,

$$g(x,z) = \frac{2}{\pi}\zeta\kappa(x,\zeta)\sqrt{1-\zeta^2}\cos\beta(x,z)$$

$$\left\{ \int_{\zeta_o=1}^{b(x)} \frac{\gamma(x,\zeta_o)\, d\zeta_o}{\kappa(x,\zeta_o)\left(\zeta_o^2 - \zeta^2\right)\sqrt{\zeta_o^2 - 1}} \right. \tag{4}$$

$$\left. + 2\int_{\zeta_o=0}^{1} \frac{F(x,\zeta_o)\cos(x,\zeta_o)\, d\zeta_o}{\kappa(x,\zeta_o)\left(\zeta_o^2 - \zeta^2\right)\sqrt{\zeta_o^2 - 1}} \right.$$

$$- F(x,\zeta_o)\sin 2\beta(x,\zeta)$$

and

$$\tan\alpha(x) + \frac{1}{\pi}\int_{\zeta_o=1}^{b(x)} \frac{\gamma(x,\zeta_o)\, d\zeta_o}{\kappa(x,\zeta_o)\sqrt{\zeta_o^2 - 1}} \tag{5}$$

$$+ \frac{2}{\pi}\int_{\zeta_o=0}^{1} \frac{F(x,\zeta_o)\cos\beta(x,\zeta_o)\, d\zeta_o}{\kappa(x,\zeta_o)\sqrt{\zeta_o^2 - 1}} = 0$$

The kappa function shown in Eq. (4) and Eq. (5) is given as,

$$\kappa(x,\zeta) = \prod_{k=1}^{N} \left| \frac{\zeta^2 - t_k^2}{\zeta^2 - t_{k-1}^2} \right|^{\frac{\beta_k(x)}{\pi}} \tag{6}$$

where $\zeta \in (0,1)$ and $t_k \in (0,1)$. The dynamic boundary condition that must be satisfied is defined as,

$$C_p(x,y,z)_{y=h} = 0 \qquad z \in [z_c, z_b], \tag{7}$$

which results in the following two relations,

$$\frac{\partial}{\partial x} z_b(x) = \frac{2V(x)v(b,x)+v^2(b,x)+w^2(b,x)+G\,h(b,x)}{2w(b,x)} \tag{8}$$

and

$$\begin{aligned} & C_p(\zeta,x) \\ & w^2(1,x) - w^2(\zeta,x) \\ & +2V(x)v(1,x) - 2V(x)v(\zeta,x) \\ & +v^2(1,x) - v^2(\zeta,x) \\ & +2\frac{\partial}{\partial x} z_c(x) \left\{ \int_{\zeta_o=\zeta}^{1} w(\zeta_o,x)\,d\zeta_o + \zeta w(\zeta,x) - w(1,x) \right\} \\ & +2z_c(x) \int_{\zeta_o=\zeta}^{1} \frac{\partial}{\partial x} w(\zeta_o,x)\,d\zeta_o \\ & +G\,h(1,x) - G\,h(\zeta,x) \end{aligned} \tag{9}$$

with non-dimensional gravity defined as,

$$G = \frac{gBc}{U^2} \tag{10}$$

where, g, is dimensional acceleration due to gravity, and B_c is the maximum full chine beam. The final relation requires that the hull surface contour match the free surface, as shown in Figure 4. This condition is referenced as the displacement continuity condition. The mathematical statement of this condition can be shown to be,

$$y_{wl}(x) = \frac{2}{\pi} \int_{\zeta_o=0}^{1} \frac{\left(h_o(\zeta_o) - \sum Hi^*\right) cos\beta(\zeta_o,x)}{\kappa(\zeta_o)\sqrt{1-\zeta_o^2}}\, d\zeta_o \tag{11}$$

The method used for satisfaction of the kinematic, dynamic, and displacement continuity conditions, as outlined in formulas (4) through (11) is described in detail in the System Solution section of Savander, et al. (2002). Force and moment equilibrium, as shown in Fig. 4 yields the following relations,

$$\begin{aligned} D_d + D_v + D_s &= T\cos(\tau+\alpha_s) \\ L_d + L_s + T\sin(\tau+\alpha_s) &= \Delta \end{aligned} \tag{12}$$

and

$$\begin{aligned} & L_d x_d + L_s x_s + D_d y_d + D_v y_v + D_s y_s \\ & + T(x_p \sin\alpha_s + y_p \cos\alpha_s) = \Delta\, T(L_{cg}\cos\tau - y_{g}\sin\tau) \end{aligned} \tag{12a}$$

All terms used in Eq. (12), and Eq.(12a) are provided in Figure 4, and are also further discussed in the nomenclature section of Savander, et al. (2002).

The relations Eq. (12), and Eq.(12a) are solved numerically for trim angle, τ, transom draft, t_d, and propulsor thrust, T, for specified vessel weight, center of gravity, and propulsion system orientation, (Δ, V_{cg}, L_{cg},α_s,x_p,y_p) for each given speed, U.

Seakeeping Analysis Methodology

The seakeeping performance, in the head sea condition, of the concepts developed in this work were analyzed with the approach originally defined

Fig. 4. Force and moment equilibrium model.

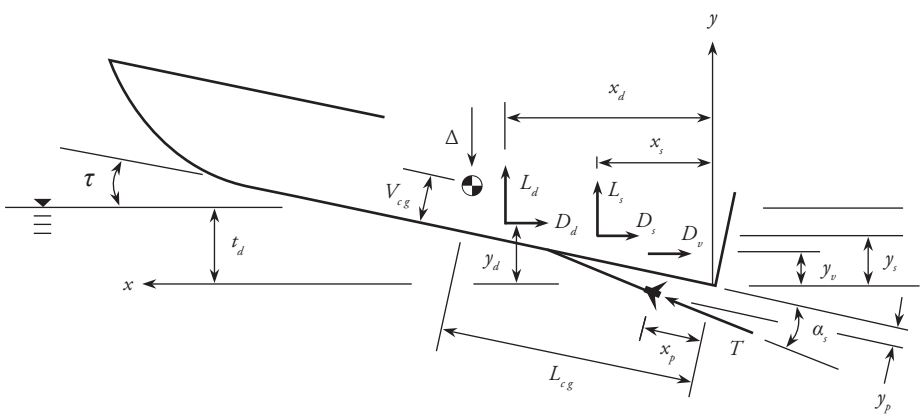

in Zarnick (1978) and (1979) and extended later by Akers et al (1999). Specifically, that method was re-created for the analysis of hull forms with longitudinal variation in deadrise travelling in regular waves. The theory is based upon utilizing a slenderness assumptions to use a combination of concepts from both strip and low aspect ratio theory. Following implementation of Zarnick (1978), the method was also extended to allow for analysis of both monohulls and multihulls in regular and random wave environments.

A theoretical summary of this formulation is provided below for convenience. Details associated with the theoretical formulation and numerical implementation are well defined in Zarnick (1978), Zarnick (1979), and Akers et al (1999) and are not repeated here.

Prediction of the rigid body motion of a high speed planing hullform operating in head or following seas is a challenging computation. The dynamic response and potentially large magnitude of the acceleration loading on the vessel structure and occupants makes this analysis of significant importance. Specifically, Zarnick (1978) highlights this point,

> "A program for planing craft would be quite useful to the small craft designer, providing a means for systematically exploring the effects of numerous design variations on performance of the craft in waves."

Further, Zarnick goes on to forsee the potential application of his method to more complex hullforms, similar to the application to trimarans, and states,

> "With minor modification, the program could also be used to examine the merits of a hybrid craft design, e.g. a combination of planing craft and hydrofoil."

Following Zarnick (1978), Figure 5 shows the coordinate system definitions utilized in the formulation. Specifically, (*x,y*) defined an inertial earth fixed coordinate system. The non-inertial body fixed system is located at the vessel center of gravity and is defined by (ξ,ζ). The vessel weight and propeller thrust is given by *W* and *T*, respectively. The hydrodynamic normal force is *N* with *D* defining the hydrodynamic drag.

Fig. 5. Seakeeping model coordinate system.

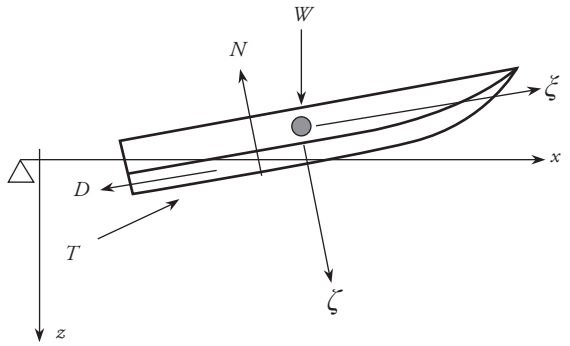

The equations of motion in the vertical plane are defined as,

$$M\frac{\partial^2 x_{cg}}{\partial t^2} = T_x - N\sin\theta - D\cos\theta \qquad (13a)$$

$$M\frac{\partial^2 z_{cg}}{\partial t^2} = T_z - N\cos\theta + D\sin\theta + W \qquad (13b)$$

and

$$I\ \frac{\partial^2 \theta}{\partial t^2} = Nx_c - Dx_d - Tx_p \qquad (13c)$$

The terms defined in Eq. (13) are given as,
M : vessel mass.
I : pitch moment of inertia.
T_x : thrust component in the x-direction.
T_z : thrust component in the z-direction.
x_c : moment arm of the normal force about the center of gravity.
x_d : moment arm of the drag force about the center of gravity.
x_p : moment arm of the propeller thrust about the center of gravity.

One of the most challenging terms to estimate in the equations of motion is the time varying hydrodynamic pressure. Integrating this pressure over the wetted hull surface at each instant in time provides, *N(t)*. Zarnick chose to use hydrodynamic impact theory of Wagner (1932) for the *N(t)* calculation, such that the vertical force per unit

length, at constant values of ξ is the body fixed system, can be defined as,

$$f = -\left\{ \frac{D}{Dt}(m_a V) + C_{D,c}\,\rho\, b\, V^2 \right\} \qquad (14)$$

where,
m_a :hull sectional, two-dimensional, added mass coefficient.
V :vertical velocity in the hull cross section plane.
$C_{D,c}$:cross-flow drag coefficient.
ρ :fluid mass density.
b :hull cross section local wetted half beam.
The added mass coefficient, following Wagner (1932), takes the following form,

$$m_a = k_a \frac{\pi}{2} \rho\, b^2 \qquad (15)$$

where k_a is an empirically determined coefficient ranging between 0 and 1. Expansion of the first term in Eq. (14) yields,

$$\frac{D}{Dt}(m_a V) = m_a \frac{\partial V}{\partial t} + \frac{\partial m_a}{\partial t} - \frac{\partial}{\partial \xi}(m_a V)\frac{\partial \xi}{\partial t} \qquad (16)$$

where the last term incorporates the ξ dependence in both m_a and V.

Fig. 6. Coordinate system used in seakeeping analysis.

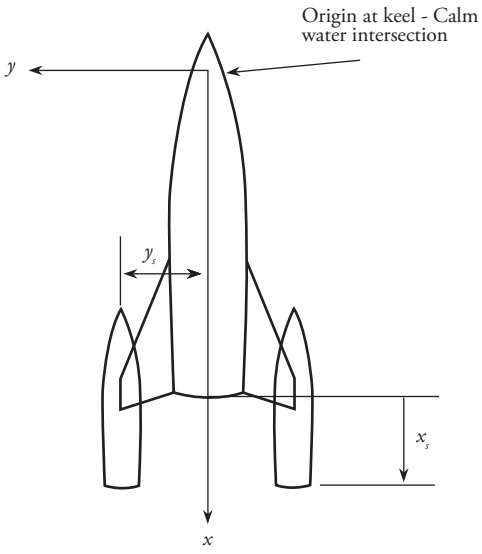

Center hull is air-transportable in a C17 and has performance specifications similar to existing monohull concepts. Wing-hulls are air-transportable in a C130 and can reach speeds of 82 knots.

The seakeeping method defined above was extended to the multihull case by allowing the three forces and three moments in the coordinate directions, (x,y,z), to be applied to the center hull. The equations of motion take the form,

$$M\frac{\partial^2 x_{cg}}{\partial t^2} = T_x - N\sin\theta - D\cos\theta + 2V_x \qquad (17a)$$

$$M\frac{\partial^2 z_{cg}}{\partial t^2} = T_z - N\cos\theta + D\sin\theta + W + 2V_z \qquad (17b)$$

and,

$$I\frac{\partial^2 \theta}{\partial t^2} = Nx_c - Dx_d + Tx_p + 2M_y \qquad (17c)$$

Note the horizontal and vertical shear forces, V_x and V_z, appear in Eq. (17). Further, the pitch moment created by each sidehull on the centerhull, M_y, is the additional term arising in the last equation of (17). The relative orientation of the sidehulls relative to the centerhull is provided in Figure 6. No hydrodynamic interaction is included in this formulation between the centerhull and sidehulls. All interaction is limited to rigid body motion modification due to force and moment transmission through the sidehull to centerhull joining structure.

Structural Design and Evaluation Methodology

Ship structures are influenced to varying levels by primary, secondary, and tertiary loading, as discussed in detail in Hughes (1988). However, loads imparted to planing hull structures are dominated by the localized dynamic loading which is associated with operation in a seaway. The localized loading causes the secondary and tertiary structural cases to drive the resulting structural design.

The general approach used in preliminary design of planing hulls is to repeatedly use strip beam theory in a static mode, as an approximation to the transient grillage - plate problem. Several papers have been authored on this topic at varying levels of rational mechanics rigor.

The dynamic load factor, *DLF*, concept requires,

$$ESL = DFL \times F_d(t) \tag{18}$$

where the dynamic load, $F_d(t)$, when multiplied by *DLF* yields the equivalent static load, *ESL*. The equivalent static load produces a static stress and strain value, $(\sigma_s, \varepsilon_d)$ such that,

$$\sigma_s = \sigma_d(t)$$
$$\varepsilon_s = \varepsilon_d(t) \tag{19}$$

where $(\sigma_d(t), \varepsilon_d(t))$ are the dynamic stresses and strains produced during transient loading. The strip beam concept utilizes one-dimensional beam elements to approximate the response of two-dimensional grillage plates via a high aspect ratio panel assumption.

This methodology of combining the dynamic load factor and strip beam theory was utilized and documented in detail in Heller and Jasper (1960). Several other authors have extended or developed similar approaches to planing hull structural design which include Allen and Jones (1977) and Spencer (1975).

Ultimately, in this study, the loading applied to the equivalent static strip beam model was approximated based upon estimation of the local acceleration and dynamic pressure magnitudes. The methods of Zarnick (1978), Zarnick (1979), and Akers et al (1999) were used to predict the vessel response and associated acceleration loading at locations of interest in the structure. The method of Heller and Jasper (1960) and Allen and Jones (1977) were used to make to the first estimate of the hull scantling plan. The resulting design was then checked against the 2001 Guide for Building and Classing High-Speed Craft published by the American Bureau of Shipping. The scantling plan was then adjusted such that ABS guide lines were met.

For this preliminary design study and ease of analysis, all hull material was assumed to be aluminum. Application of fiberglass and composite technology to this design may be very attractive from a strength to weight perspective and should be evaluated in future design work.

Multi-Hull Concept Selection

As mentioned in earlier sections, both trimaran and catamaran concepts were considered. The trimaran configuration was selected over a catamaran vessel for three primary reasons: air-transportability, modes of independent operation, and seakeeping performance.

The catamaran concept is based upon joining two 80 ft vessels with a common deckhouse structure that spans between the two hulls. Air-transport would be performed with a pair of C17 aircraft. The deckhouse structure would also have to be removable and packaged for air transport with the side hulls. Unlike the trimaran, the catamaran design does not readily allow each sidehull to operate in an independent mode. Once the sidehulls are joined together no convenient mode of independent operation exists unless the joining structure is completely jettisoned.

The trimaran concept, as shown in the sketch in Fig, 6, would use wing structures to join the 80 ft. center monohull to two 40 ft. wing units. The wing units are air-transportable in a C130 aircraft with the centerhull being transportable in a C17. The wing and center units are all capable of independent operations and missions. The centerhull can operate without the wing units and with the wing structures stored in a retracted mode.

C130 aircraft are more readily available to the SOF than C17 aircraft. As a result, the trimaran concept is more desirable from the air-transport perspective. The trimaran also exhibits advantages over the catamaran in that each of the trimaran component hulls are capable of independent modes of operation.

In addition to air-transportability and independent modes of operation of the component hulls, the trimaran offers the ability to increase the effective length of the craft by giving the wing units an aft longitudinal bias. This bias effectively increases

the length to beam ratio of the combined vessel, when compared to the center monohull alone, in a head sea condition. The net result is a vessel with improved seakeeping response over the monohull. The catamaran does not have this attribute.

Trimaran Concept Development

The design approach for the trimaran concept was to modify a monohull concept similar to the existing Mark V and incorporate two detachable wing hulls, as shown in Fig. 6. A main feature of the design is the aftward longitudinal location of the wing hulls relative to the center hull. This aftward movement of wing units results in an equivalent monohull with an increased length to beam ratio, *L/B*, when compared to only the centerhull (Fig. 7). An increase in the effective *L/B* ratio, when exposed to a head sea condition, results in improved dynamic response of the vessel.

The wing units are powered to have an independent top speed which is more than 50% greater than the top speed of the center hull. Hence, the wing units can be considered propulsion booster units that offer an increased speed capability compared to the sole center hull. With the added power, the trimaran high speed platform is designed to allow the SOF to travel faster and with less fatigue when compared with traditional 80 ft class monohull designs.

The trimaran design also emphasizes the integration of several vessels similar in characteristics to the current SOF fleet including, Mark V, HSAC, RHIB, CRRC, and PWC, into one common high speed platform. The detachable wing units shown in this figure, similar in size to the current HSAC, could be capable of both manned and unmanned modes of operation.

It is expected that unmanned platforms will become more in demand as the requirements for vessel operations in environments not limited by human exposure increase (e.g. Cooper and Norton (2002)). Sokel and Hansen (2001) cite Senator Warner of Virginia challenge to Congress in 2000-2001 to significantly increase plans for buying and developing unmanned systems. Further, Sokel and Hansen (2001) go on to quote the Director of Naval Operations and Strategic Studies group stating that within 50 years 75% of all ship sensors and weapons will be remote.

Trimaran Preliminary Concept Design Details

As mentioned previously when considering relative merits of trimaran's and catermarans, the aftward movement of side-hulls results in an equivalent monohull with an increased length to beam ratio, *L/B*, when compared to only a single center-hull (Fig. 7). Specifically, given a monohull of length overall, $L_{monohull}$, with two side-hulls attached such that the transom of the side-hull is x_s feet aft of the transom of the monohull, the effective length of the trimaran becomes,

$$L_S = L_{monohull} + x_S \tag{20}$$

In a head sea condition, the trimaran acts effectively as a lengthened monohull via,

$$\frac{L_e}{B} > \frac{L_{monohull}}{B} \tag{21}$$

also shown in Fig. 7. This effective increase in the length to beam ratio has favorable implications on seakeeping performance. The position of the side-hull relative to the center-hull is defined by the coordinates, (x_s, y_s), Fig 6. The effect of the side-hull position on the vertical acceleration experienced at the center of gravity, CG, and the bow of the craft is provided in Fig. 8.

Figure 8 shows that nearly a factor of two reduction in bow acceleration can be achieved by moving side-hull position from $x_s = 0ft$ to $x_s = 20ft$. The data provided corresponds to operation in sea state 3 at a speed of 50 knots for a 5 minute exposure period.

Bow and CG acceleration seakeeping results for a specific value of $x_s = 15ft$ and a range of sea states are also shown in Fig. 9. This figure also shows a significant improvement in seakeeping qualities of the trimaran over the monohull design from both a maximum perspective. All results shown in

Fig. 7. Conceptual illustration of how side-hulls in a trimaran concept produce an effective monohull with an increased length to beam ratio.

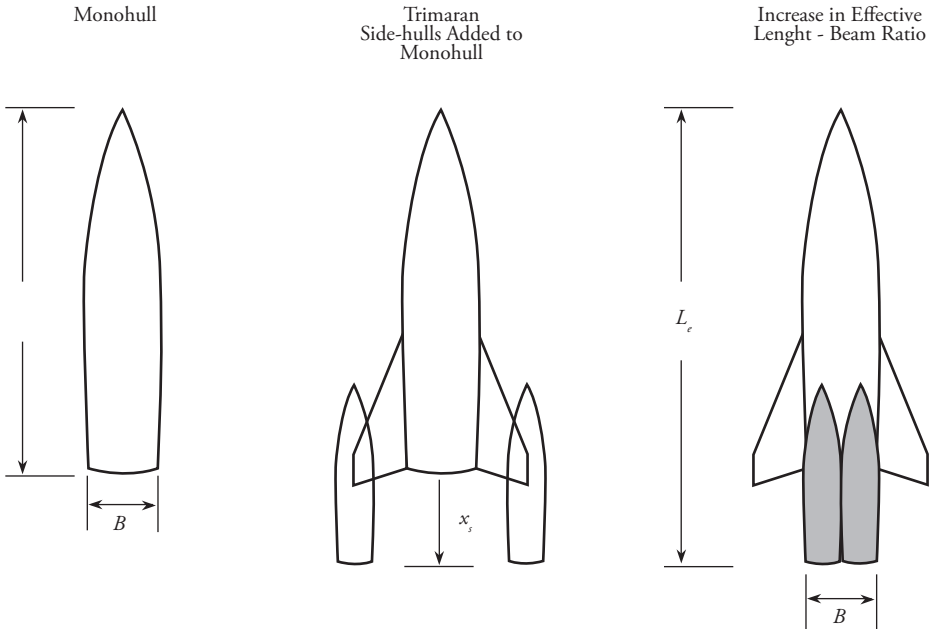

Fig. 8. Bow and CG acceleration response to variation in longitudinal position of side-hulls relative to center-hull. Exposure limit for the computation was 5 minutes. The speed was 50 knots and the sea conditions were sea state 3

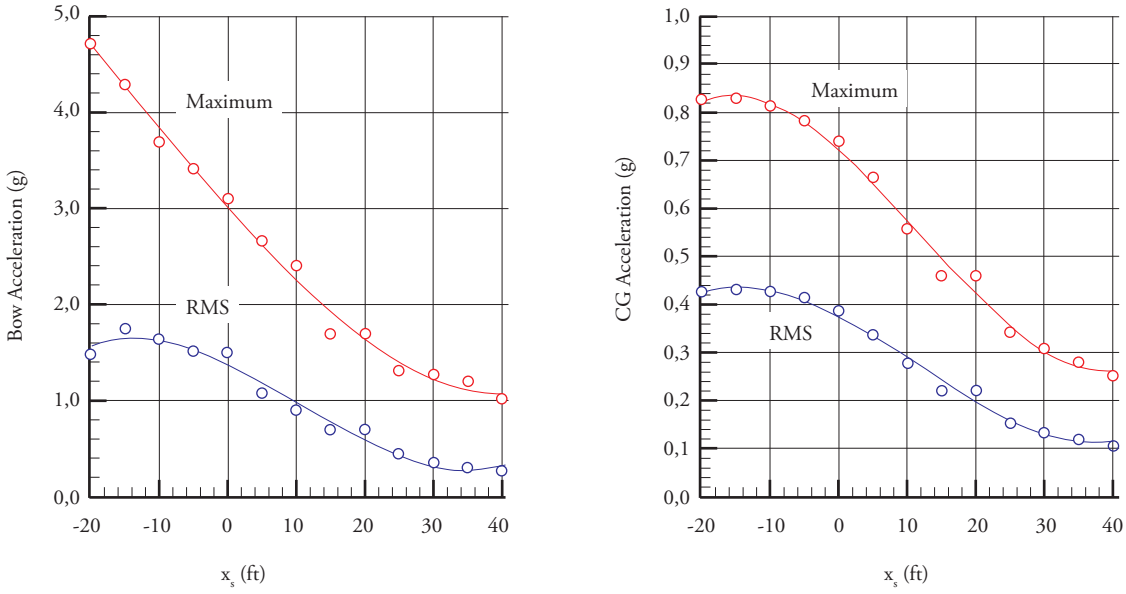

these two figures were for a 3-hour exposure while operating at 50 knots in sea state 3.

As a result of this preliminary seakeeping analysis, trimaran designs were developed with a side-hull position range defined by,

$$\begin{matrix} x_S \in (15,20)\, ft \\ y_S \in (15,25)\, ft \end{matrix}. \qquad (22)$$

The initial trimaran design was considered with the side-hull position of,

$$\begin{matrix} x_S = 20\, ft \\ y_S = 25\, ft \end{matrix}. \qquad (23)$$

This transverse spacing coupled with the large vertical load imparted by the side-hull at the end

Fig. 9. Bow and CG maximum acceleration response as a function of sea condi-tions. The side-hull transom was 15 feet aft of the center-hull transom, $x_s = 15ft$. All computations were based on a 3-hour exposure at a speed of 50 knots.

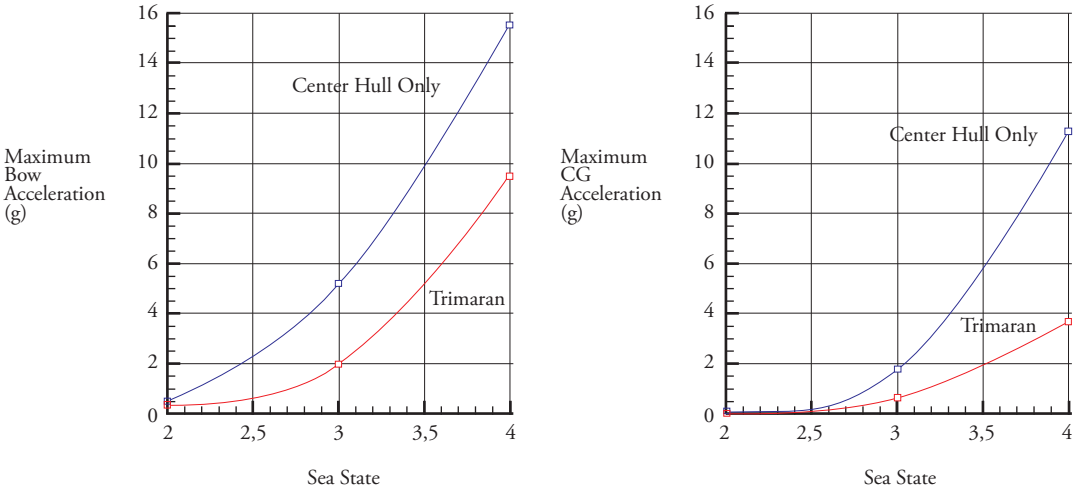

Fig. 10. Bow and CG RMS acceleration response as a function of sea conditions. The side-hull transom was 15 feet aft of the center-hull transom, $x_s = 15ft$. All computations were based upon a 3-hour exposure at a speed of 50 knots.

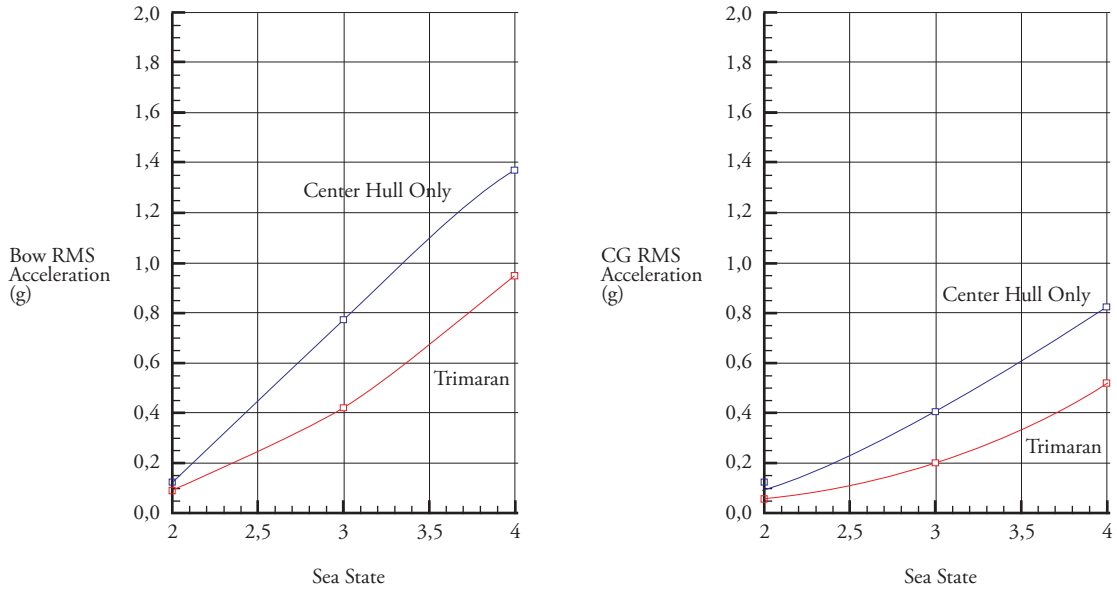

of the wing structure, proved to make this version of the design unfeasible. The structure needed to carry the load became too large with evaluated against weight constraints.

As a result, the position of the side-hulls was moved closer to the center-hull with,

$$\begin{matrix} x_S = 15\,ft \\ y_S = 18\,ft \end{matrix} \quad . \qquad (24)$$

as shown in Fig. 11. The total length and beam for the trimaran concept is 94 feet 3 inches and 46 feet 1 inch, respectively. The total displacement is approximated at 59 long tons. The top speed for this design is estimated to range between 56 to 62 knots. This represents a 4 to 10 knot increase in the top speed over an equivalent monohull concept.

The side-hull design consists of two craft approximately 40 feet in length with beams of 9

feet 3 inches. These craft have displacements of 13,000 lbs and top speeds of 82 knots.

Each vessel is powered by twin SeaTek 10.3 Endurance diesels each driving Arneson surfacing systems. A fuel capacity of 400 US gallons allows a range of 540 nautical miles at a cruise speed of 50 knots. The range at a maximum speed of 82 knots is reduced to 200 nautical miles. The hulls are expected to be constructed of a composite based fiberglass reinforced plastic (FRP).

The total concept range is calculated to be 600 nautical miles at a cruising speed of 40 knots. A range of 540 nautical miles is maintained at 50 knots, with the range dropping to 220 nautical miles for the top speed condition. The range is reduced at top speed due to the full power demand on the four SeaTek diesels located in the side-hulls at this operating point. The total fuel capacity is 4,400 US gallons representing the summation of 2,600 US gallons for the center-hull and 800 US gallons for the two side-hulls combined.

Fig.11. Trimaran concept showing modified wing structure. Position of side-hulls rela-tive to the center-hull has been reduced both transversely and longitudinally based upon transient structural analysis with operation at 50 knots in sea state 3. Center hull is air-transportable in a C17 and has performance specifications similar to existing monohull concepts. Wing-hulls are air-transportable in a C130 and can reach speeds of 82 knots.

LOA: 94 feet 3 inches
Beam: 46 feet 1 inch
Max. Speed: 56 - 62 kts
Cruise Speed: 40 kts
Payload: 8,400 lbs (approx.)
Range: 600 NM at 40 kts, 540 NM at 50 kts
Range at Max Speed: 220 NM

Engines: 4 x 1050 HP SeaTek 10.3
Endurance: 2 x 2285 HP MTU 12V4000
Drives: 4 x Arneson Surfacing Drives
KaMeWa K50s Watejets
Fuel: 4,400 US Gal
Hull Material: Aluminum & FRP
Displacement: 58.8 LT (approx.) 2 x

Trimaran Steady Hydrodynamic Analysis

The methods described in steady planing and seakeeping sections were used to design the hullform for the side-hull in the trimaran concept. The final side-hull craft is shown in Figures 11 and 12. Additionally, the analytical extension to Zarnick (1978) and Akers et al (1999), as defined in was also extended to compute the steady resistance and equilibrium position of the trimaran concept as a function of forward speed. This section of the report documents the design and performance of the independent side-hull hullforms and the trimaran concept.

The non-dimensional longitudinal coordinate of the hullform is given by,

$$\xi = \frac{x}{z_{ch}} \tag{25}$$

where z_{ch} is the maximum chine half beam. The deadrise at the transom is 20 degrees and is maintained to a value of ξ = 1,5 at which point the deadrise increases to a value of 55 degrees at the chine-keel intersection. The maximum chine

Fig. 12. Lines plan for the side-hull of the trimaran concept

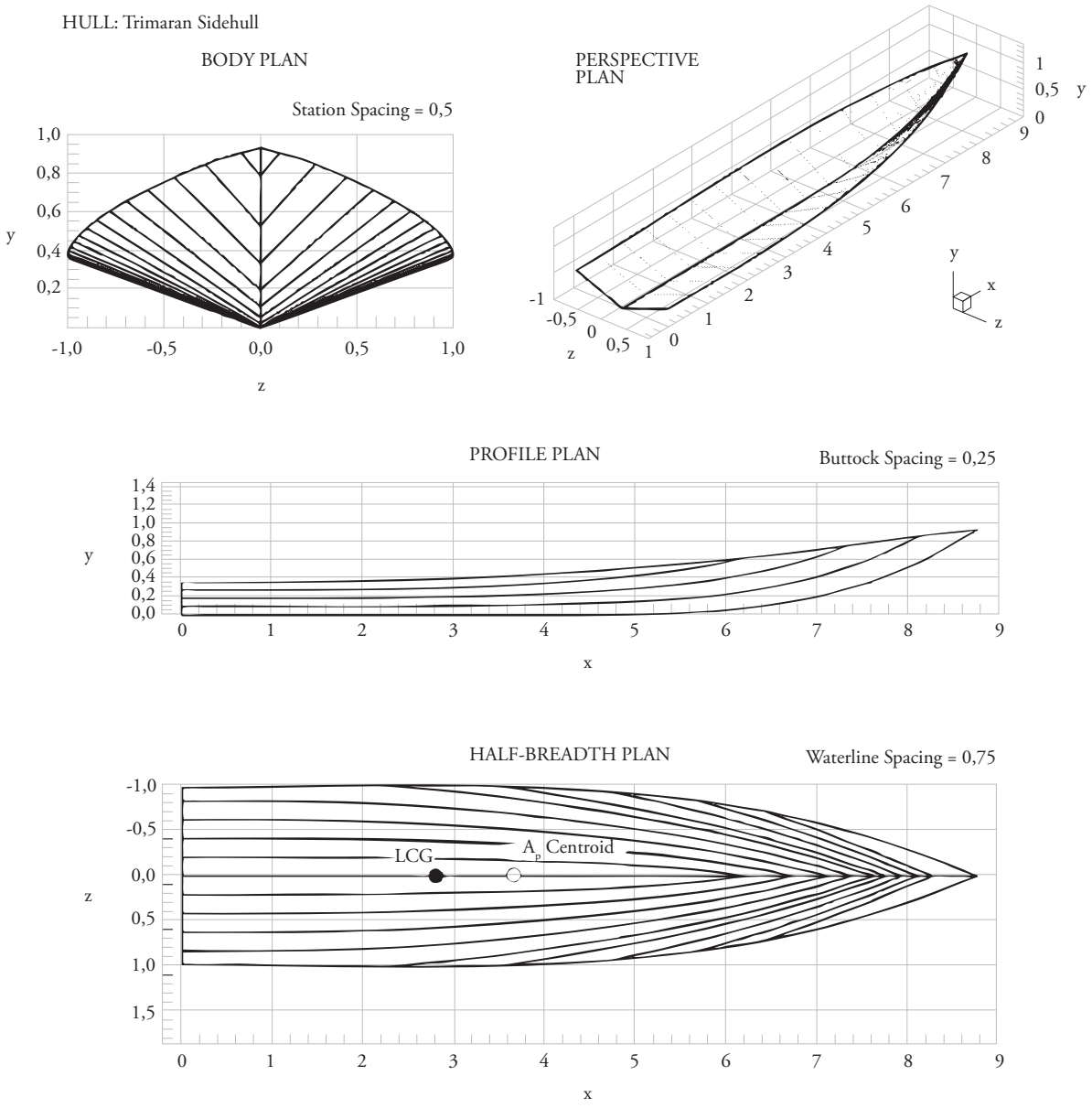

beam is located at ξ = 3,0 and is approximately maintained aft to the transom. The keel contour is flat from the transom to ξ = 5,0 where the keel elevation begins to increase to the maximum value of approximately,

$$\frac{y}{z_{ch}} = 1{,}0 \qquad (26)$$

at the chine-keel junction. The hullform planing surface is defined by the deadrise distribution, chine beam distribution, and keel elevation. The lines plan, consisting of the body, plan, and profile views is shown in Figure 12. The centroid of the planing area, A_p, is located,

$$\frac{x_{A_\gamma}}{z_{ch}} = 1{,}0 \qquad (27)$$

with the longitudinal center of gravity position being,

Fig. 13. Trimaran concept side-hull corresponding to F_∇= 4,0 (32.7 kts). Plots include a) total pressure coefficient, b) sectional dynamic and static lift coefficient, and c) velocity vector and streamline orientation. *(x,y,z)* coordinates are nondimensionalized by maximum chine half-beam, Z_{ch} . Note the extent of chines-wet flow.

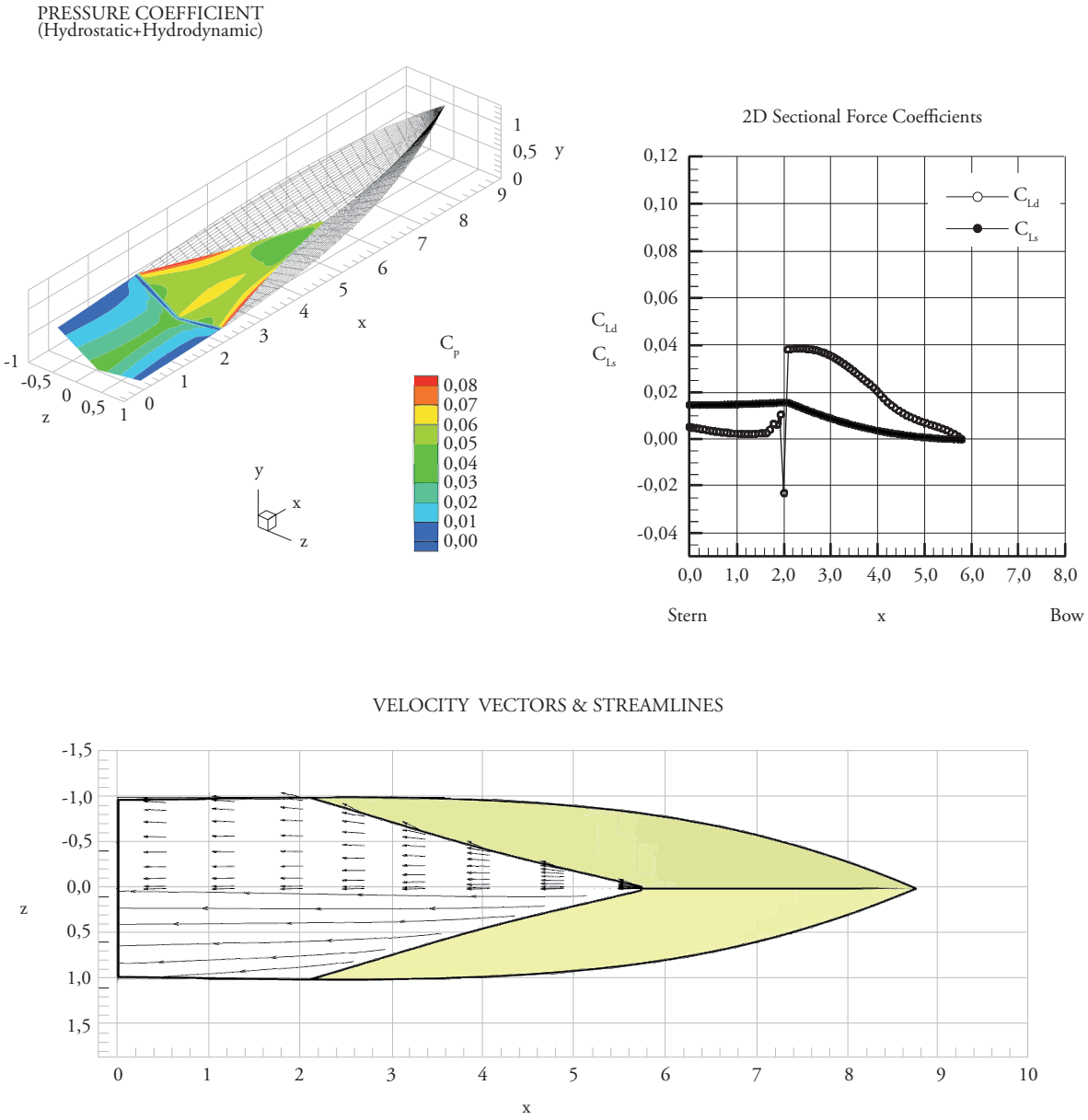

$$\frac{L_{cg}}{z_{ch}} = 2{,}75 \qquad (28)$$

forward of the transom. The length of the planing surface, L_p, is 35 feet. The centroid of the A_p is 41.7% forward of the transom with the L_{cg} located a distance of 10% of L_p aft of the A_p centroid.

Results of the steady hydrodynamic analysis for the side-hull hullform are provided in Figures (13) through (15). These figures correspond to a volumetric Froude number,

$$F_\nabla = \frac{U}{\sqrt{g\nabla^{1/3}}} \qquad (29)$$

ranging from 4.0 to 12.0. The associated speed ranges from 32.7 knots to 98.0 knots.

Fig. 14. Trimaran concept side-hull corresponding to $F_\nabla = 10{,}0$ (81.7 kts). Plots include a) total pressure coefficient, b) sectional dynamic and static lift coefficient, and c) velocity vector and streamline orientation. *(x,y,z)* coordinates are nondimensionalized by maximum chine half-beam, Z_{ch} . Note the extent of chines-wet flow.

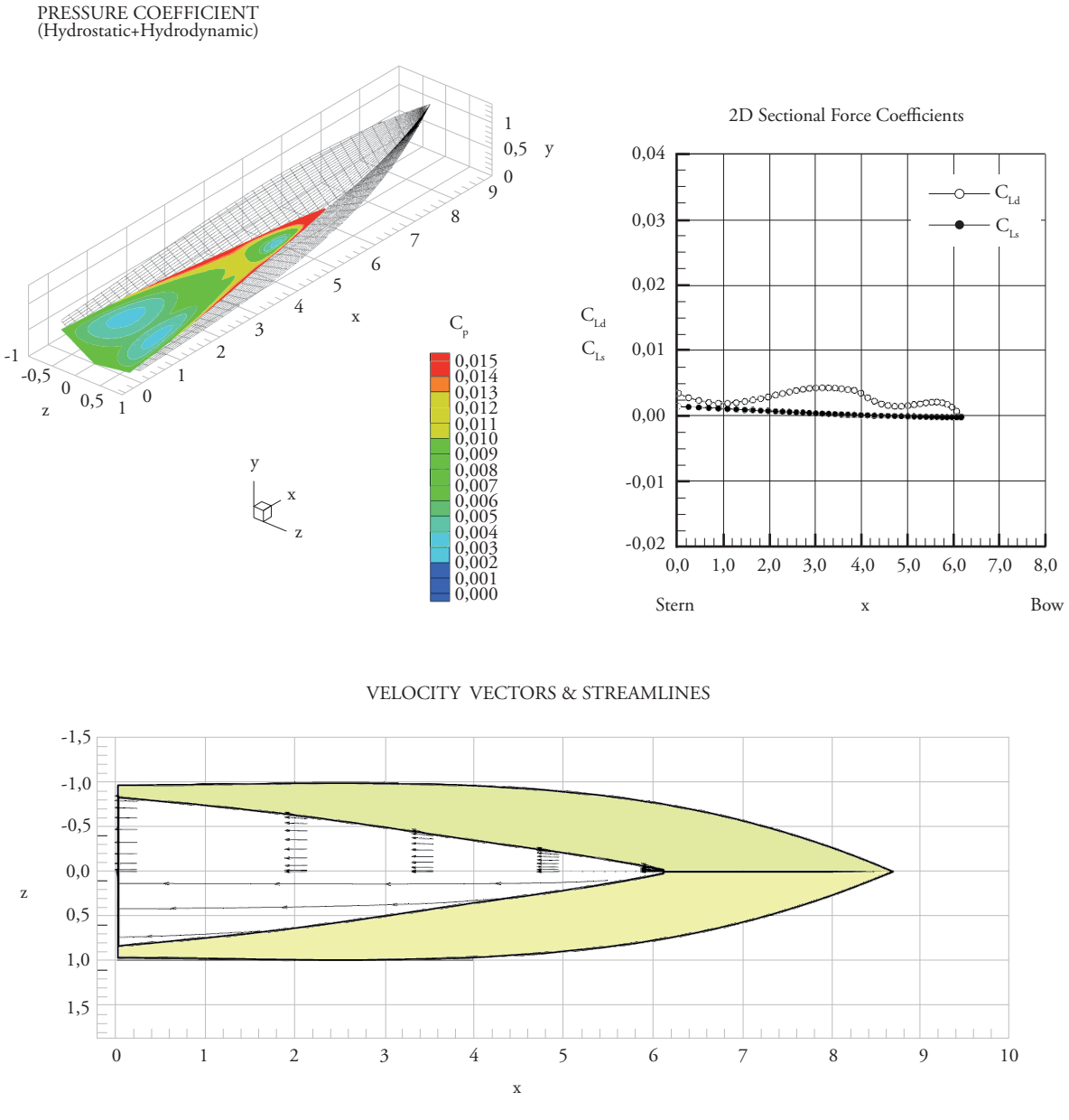

Fig. 15. Side-hull lift and drag coefficient as a function of F_∇

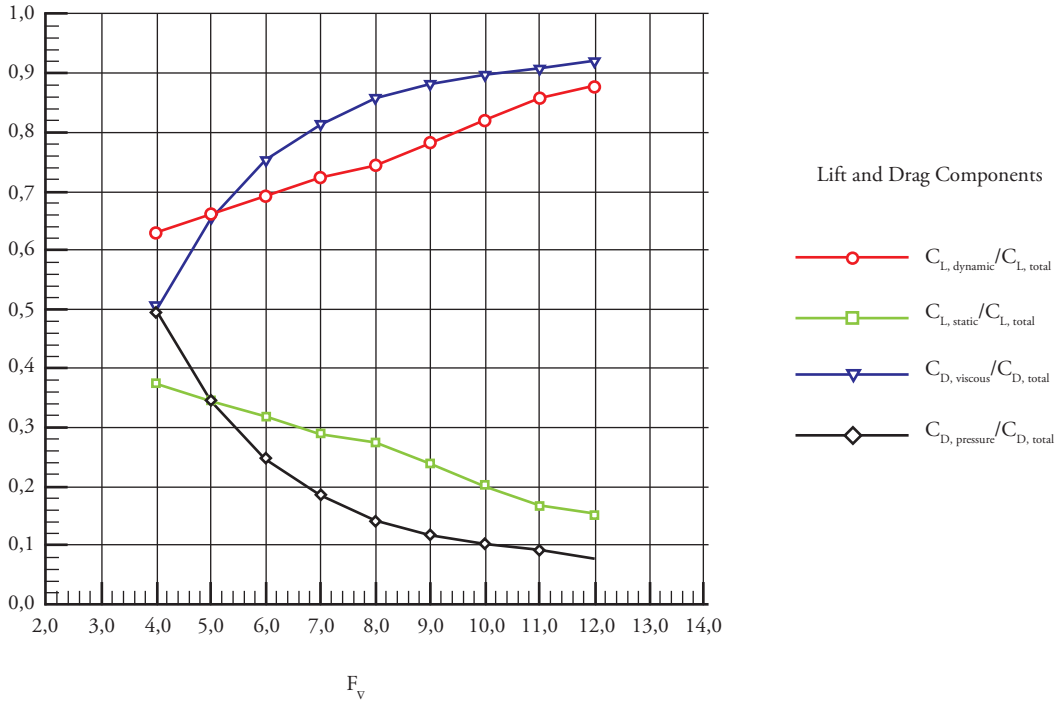

The total pressure coefficient is defined as,

$$C_p = \frac{P}{\frac{1}{2}\rho U^2} \tag{30}$$

with the sectional, two-dimensional, force coefficients given by,

$$C_{L_d} = \frac{P_d}{\frac{1}{2}\rho U^2 B} \qquad C_{L_s} = \frac{P_s}{\frac{1}{2}\rho U^2 B} \tag{31}$$

The hydrodynamic and hydrostatic lift force per unit length of the hull are L_d and L_s, respectively. The entire wetted planing surface is comprised of the chines-dry flow phase at a F_∇ = 8 or 65.3 knots. At this speed, no chines-wet phase is present.

Figure 15 shows the contribution of hydrodynamic and hydrostatic lift as a percentage of total lift for varying volumetric Froude number. Similarly, the percentage of viscous and pressure drag of the total drag is also shown in this figure. At a F_∇ = 4 (32.7 knots) the lift ratios are,

$$\frac{C_{L,\,dynamic}}{C_{L,\,total}} \cong 0{,}62, \tag{32a}$$

$$\frac{C_{L,\,static}}{C_{L,\,total}} \cong 0{,}38. \tag{32b}$$

and at F_∇ = 12 (98.0 knots) these ratios become,

$$\frac{C_{L,\,dynamic}}{C_{L,\,total}} \cong 0{,}86, \qquad \frac{C_{L,\,static}}{C_{L,\,total}} \cong 0{,}14. \tag{33}$$

At 32.7 knots the pressure and viscous drag components are nearly equivalent. However, at top speed of 98.0 knots, the viscous drag dominates the total drag as shown by,

$$\frac{C_{D,\,viscous}}{C_{D,\,total}} \cong 0{,}92, \qquad \frac{C_{D,\,pressure}}{C_{D,\,total}} \cong 0{,}08. \tag{34}$$

This illustrates how any method, such as bubble drag reduction or hull steps, can have a potentially large influence on the top speed of the craft in this Froude number range.

Figure 16 illustrates the contribution to lift and drag from the chines-dry and chines-wet flow

Fig. 16. Side-hull lift and drag contribution for chines-dry and chines wet flow phases as a function of F_∇

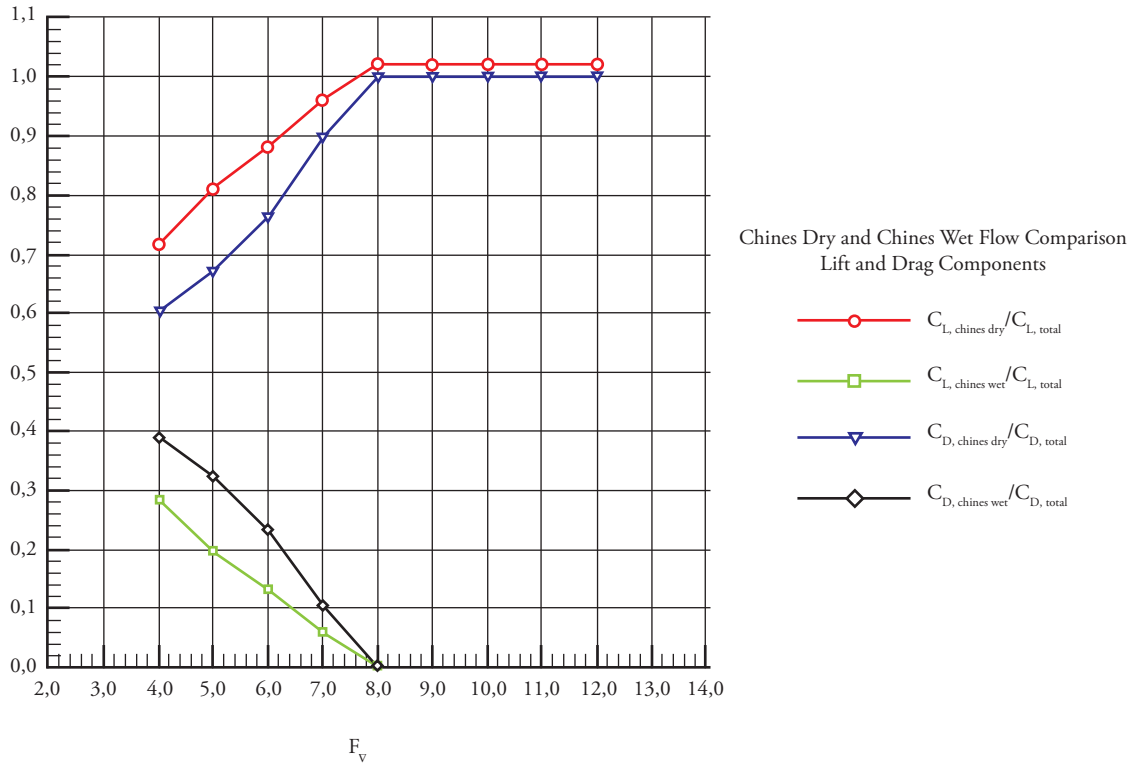

regimes as a function of F_∇. This figure shows that the CW flow phase is completely avoided at $F_\nabla = 8$ and how the majority of lift and drag is associated with the CD area.

The resistance to displacement ratio is defined as,

$$\frac{R_t}{\Delta} \tag{35}$$

The combined performance of the monohull and two side-hulls for the trimaran concept is shown in Figure 17. The monohull, trimaran, and trimaran (MOD1), are depicted in this figure. The monohull curve is the same curve shown in of the monohull hydrodynamics section. The trimaran curve (blue line) is the steady BHP required at each speed computed by satisfying the vertical plane equations, through, in the following modified form,

$$\begin{aligned} 0 &= T_X - N\sin\theta - D\cos\theta + 2V_X, \\ 0 &= T_Z - N\cos\theta + D\sin\theta + W + 2V_Z, \end{aligned} \tag{36}$$

and

$$0 = Nx_C - Dx_d + Tx_p + 2M_y.$$

The acceleration terms on the left hand-side of all equations is set to zero for the steady case. Figure (17) shows that the maximum speed for the monohull alone is 51.9 knots given a total BHP available of 4,570 hp. The total power available in the trimaran configuration from two MTU 12V4000 and four SeaTek 10.3 Endurance diesels is 8,770 hp. The trimaran curve (blue line) indicates that the top speed in the trimaran mode increases to 56 knots from 51.9 knots for the monohull case.

Aft positioning of the side-hulls with positive x_s values tends to cause a net reduction in operating trim angle when compared with independent monohull operation. This reduction in trim magnifies the viscous drag penalty. Hence, stepped planing hulls or drag reduction methods, have the potential to increase the attainable top speed for the trimaran. An estimate or upper bound for this speed increase can be approximated by adding the BHP requirement for the monohull and side-hull component when each hull is operating in an independent mode. Adding the BHP curves provided in Figure 17 yields the green curve

Fig. 17. Comparison of monohull and trimaran BHP requirements

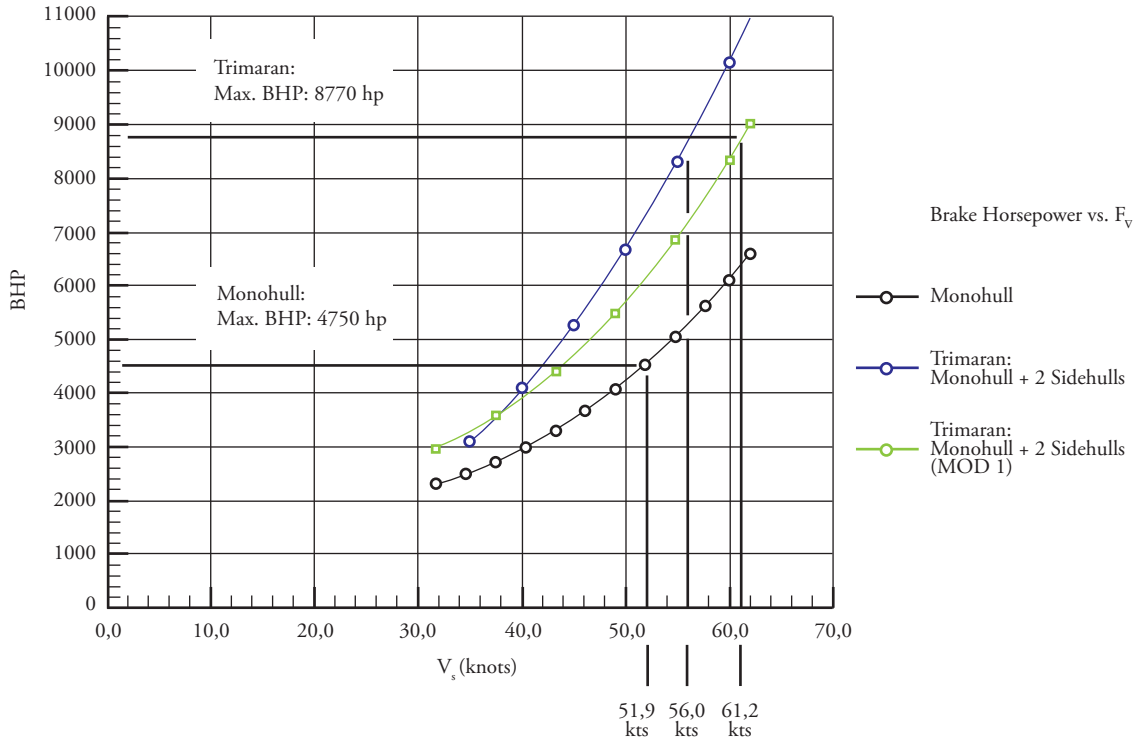

labeled "Trimaran: (MOD1)." This curve shows the top speed for the trimaran concept increasing to 61 knots and yielding a 9-knot increase when compared to the monohull case.

Hence, the trimaran concept provides a 4 to 9-knot potential increase in top speed when compared to operation of the monohull alone.

Trimaran Seakeeping Analysis

A seakeeping analysis is documented in this section for the trimaran concept. The concept consists of joining two side-hulls to a center-hull via a wing structure connection as is described in the concept development discussion. The methods defined by Zarnick (1978), Zarnick (1979), and Akers et al (1999) have been extended and generalized to allow for computation and analysis of planing multi-hull configurations.

Table 2 defines the combination of craft speeds and sea conditions analyzed in this study for the trimaran. All results shown reflect a 3-hour exposure period. Table 2 shows that no bow acceleration exceeds 2.5 g for the trimaran case at the speeds analyzed of 25, 50, and 60 knots, with operation in sea state 2 or 3. Further, for the trimaran, no CG acceleration exceeds 1 g while operating at 35, 50, or 60 knots in sea state 2 or 3. However, the monohull predictions show bow acceleration values of 4 to 5 g for these same cases. The maximum acceleration values for the CG and bow have also been plotted for both the trimaran and monohull for the 50 knot case in Figures 18 and 19.

Figures 18 and 19 show a comparison of trimaran and monohull response to the same wave elevation time history. These plots show a portion of a 3-hour simulation for the vessels operating at 50 knots in sea state 4. Sea state 4 has a significant wave height of 6.2 feet. The time histories plotted show the maximum value for the monohull operating without the side-hulls. The green lines show the response of the trimaran to this same wave elevation excitation. These results highlight the significant reduction in vertical acceleration experienced at both the CG and bow of the trimaran when compared with the monohull case. Specifically, a

Table 2. Trimaran Seakeeping Maxima Results for a 3-Hour Exposure Period

			Trimaran		Monohull	
Speed (kts)	**Sea State**	**Location**	**Max**	**RMS**	**Max**	**RMS**
35	2	Bow	**0.27**	0.0.71	0.38	0.123
35	2	CG	**0.08**	0.022	0.12	0.035
35	3	Bow	**1.64**	0.338	4.42	0.610
35	3	CG	**0.39**	0.135	1.63	0.272
35	4	Bow	**8.03**	0.687	14.75	1.135
35	4	CG	**2.49**	0.338	7.57	0.638
50	2	Bow	**0.36**	0.088	0.50	0.136
50	2	CG	**0.11**	0.031	0.18	0.045
50	3	Bow	**1.98**	0.417	5.17	0.773
50	3	CG	**0.71**	0.191	1.83	0.398
50	4	Bow	**9.49**	0.924	15.54	1.342
50	4	CG	**3.68**	0.516	11.37	0.837
60	2	Bow	**0.42**	0.099	0.51	0.146
60	2	CG	**0.14**	0.038	0.22	0.052
60	3	Bow	**2.53**	0.510	4.18	0.836
60	3	CG	**1.02**	0.250	1.77	0.459
60	4	Bow	**10.75**	1.086	- - -	- - -
60	4	CG	**4.7**	0.639	- - -	- - -

Fig. 18. Monohull and trimaran bow vertical acceleration time history comparison.
The maximum values for a 3-hour exposure operating at 50 knots in sea state 4 are shown

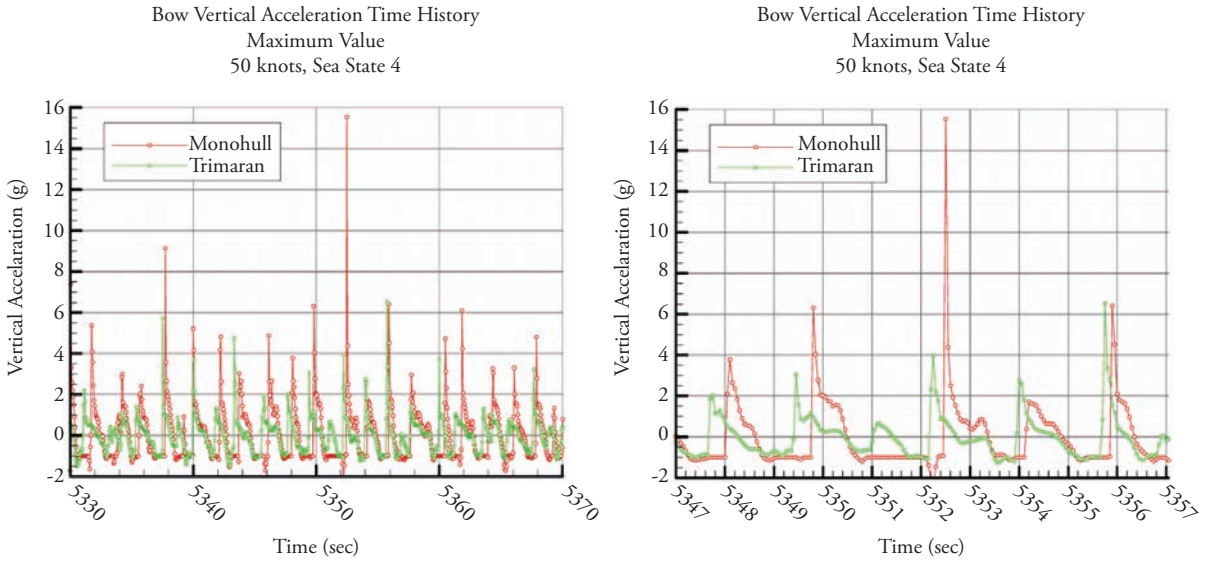

maximum bow acceleration of over 15 g is predicted for the monohull in these conditions. The trimaran bow acceleration is predicted to be only 4 g. The maximum CG acceleration computed is nearly 12 g for operation in sea state 4 at 50 knots for 3 hours for the monohull. The trimaran concept experiences a CG vertical acceleration of only 2 g in these same conditions.

Fig. 19. Monohull and trimaran CG vertical acceleration time history comparison.
The maximum values for a 3-hour exposure operating at 50 knots in sea state 4 are shown

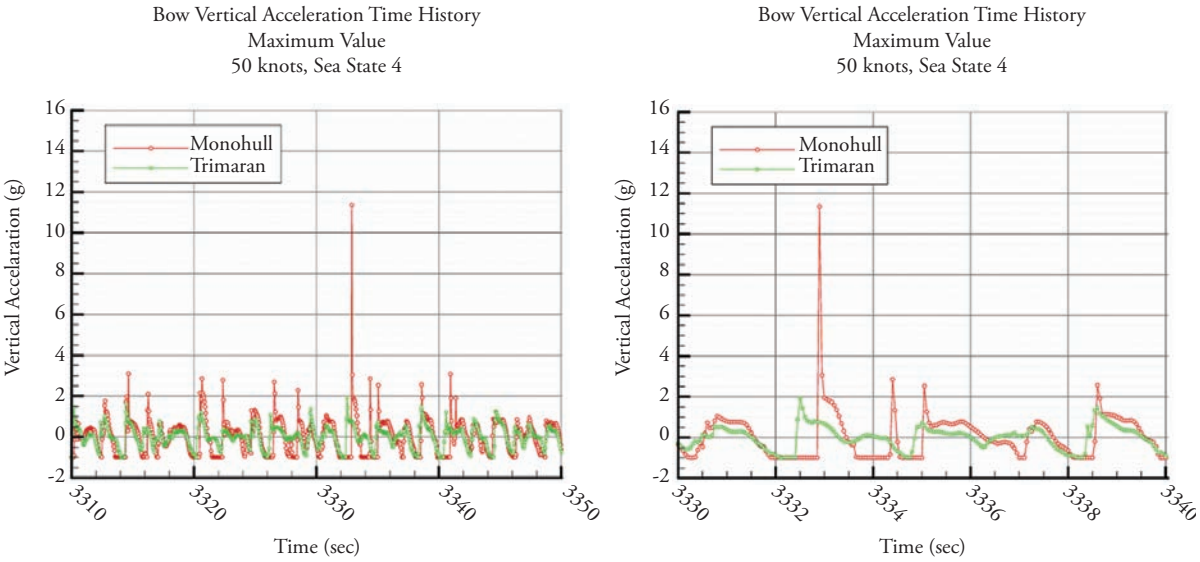

Fig. 20. Perspective view of space frame structure designed to carry side-hull loading.
Structural design is shown from transom to forward engine room bulkhead

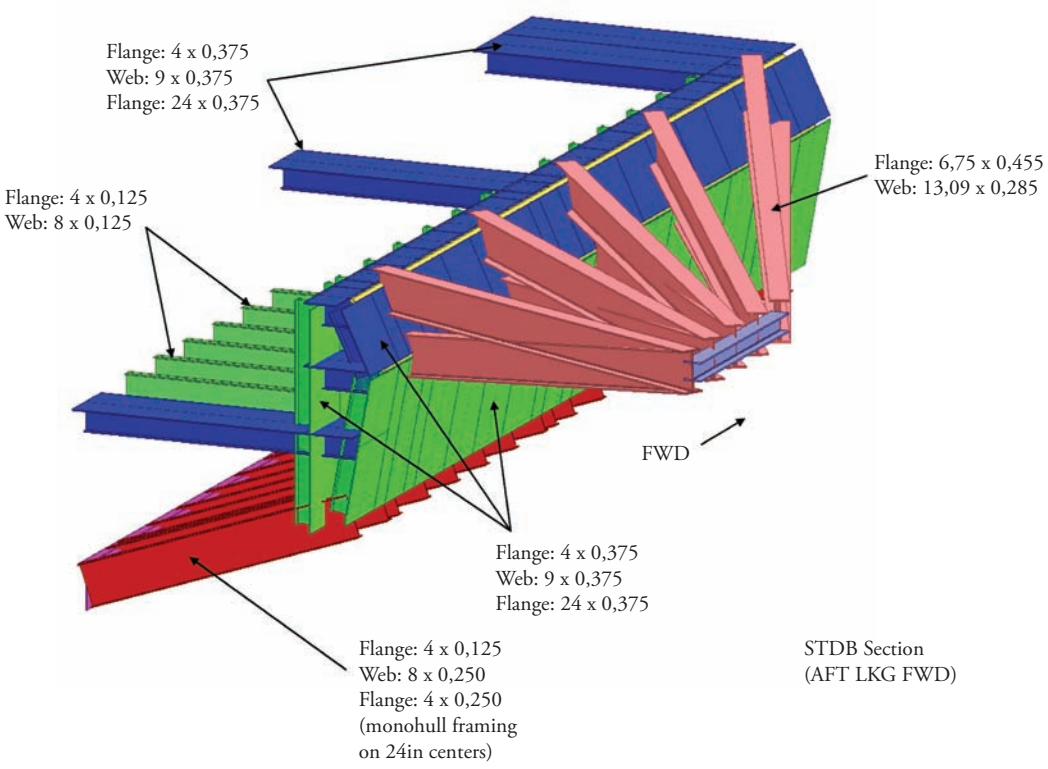

Trimaran Structural Design and Evaluation

One of the main challenges with the trimaran concept is the structural design. The structure must be able to withstand a transient loading environment generated by operating at high speed in a seaway. This environment imposes high levels of stress throughout the entire hull. Further, the transient nature of the seaway generated loads also causes the structure to endure several loading and unloading cycles. Hence, this can be considered both a high-stress and high-cycle structures problem.

The analysis contained in this section consists of designing a space frame structure for two load cases. The first load case is static suspension of the entire 13,000-pound side-hull from the center-hull. The second load case corresponds to the maximum vertical transient force generated by operation of the trimaran system at 50 knots in sea state 3 over a 3-hour duration period. This results in a maximum load pulse with an amplitude of 70,000 lbs and a pulse width of approximately 1,000 milliseconds (1.0 seconds).

The space frame structure designed to withstand this loading environment is provided in Figure 20. Due to the severity of the transient load case, the size of several of the monohull members had to be increased. Additionally, the transverse frame spacing was reduced aft of the engineroom bulkhead from 48 inches for the monohull case to 24 inches for the trimaran center-hull structure.

The aft cargo bay and engine room access have been maintained. The loading impulse utilized in this analysis is given by,

$$V_z(t) = A\sin^2\left(\frac{\pi t}{T}\right) \qquad (37)$$

where $A = 70.000lbs$

Each of the members defined in Figure 20 were modeled as beam columns. The structural dynamics problem was solved using a transient finite element analysis (FEA) solver where both forces and moments are transferred at FEA joint locations. Zero displacement and zero slope boundary conditions are maintained along the centerline of the structure.

The increase in size of scantlings aft of the engine room bulkhead has been significant. The weight of the wing structure is 10,144 pounds. The weight aft of the engine room bulkhead for the center-hull becomes 20,288 pounds. The weight aft of the engine room bulkhead for the monohull design is only 6,210 pounds. Hence, the weight penalty added to convert the monohull concept into the center-hull of the trimaran concept is 14,078 pounds.

Table 3 shows the monohull weight estimate modified to include the additional wing structure. The total weight of the center-hull has increased from 98,974 pounds for the monohull to 113,052 pounds for the center-hull. This increase of 14,000 pounds in weight is significant. However, assuming that the loading coefficient of,

$$\frac{A_p}{\nabla^{2/3}} = 6.2 \qquad (38)$$

is acceptable, as discussed in connection with formulas through, the total displacement of center-hull in a loading configuration similar to the current Mark V would be approximately 127,000 pounds. This displacement estimate for the center-hull still allows for a 14,000 pound contingency in the weight estimate.

The results of this section underscore the challenging nature of designing a structure to withstand the transient load environment encountered by high speed planing hulls operating in sea state 3 and above. The weight implications of the additional structure have been shown to be significant, but they may be within reasonable bounds from a loading coefficient perspective.

Summary

Design Summary

A design study has been completed for a mission configurable combatant craft. Several different

Table 3. Monohull preliminary weight estimate with wing structure

Description	Unit Weight	Qty	Total (lbs)
Aluminum Structure	13,801 lbs.	NA	13,801
Engines: MTU 12V 4000, with gears & fluids	16, 620 lbs	2	33,240
Waterjets: KaMeWA K50s	1,941 lbs	2	3,882
Diesel Fuel	8.5 lbs/US Gallon	2,600	22,100
Fresh Water	10.0 lbs/US Gallon	250	2,500
Gray Water	10.0 lbs/US Gallon	250	2,500
Outfitting: All systems.	75% of Alum. Struct. Weight.	NA	10,351
Crew:	350 lbs/crew	16	5,600
RHIB	2,500 lbs	2	5,000
Wing Structure	14,078 lbs	1	14,078
		Total:	**113,052**

concepts have been evaluated. Each concept was air-transportable and readily reconfigurable to meet a broad range of mission demands. Two design themes emerged in the process of completing this work. One centered around a technically conservative monohull concept which provided capabilities and performance similar to current SOF craft and the second centered around a multi-hull concept that exhibited significant technical risk, but offered significant operational and vessel performance enhancements.

Monohull: All design and analysis work for the monohull concept which included potential modifications to the current Mark V craft, centered around air-transportability in a C17 cargo plane. Modularity of the monohull concepts were not pursued since the C17 cargo volume is very similar to the dimensions required for an 80-foot, 50-knot planing hull. Hence, there was no need to subdivide into modules a new monohull design that had dimensional particulars similar to the current Mark V. However, the height of the Mark V was determined to be the main geometric constraint with air-transportation in a C17. Proposed modifications included to permanently lower the current hardtop deckhouse by lowering the main deck beams in way of the deckhouse or remove the current deckhouse hardtop and replace it with a collapsible canvas top and clear enclosure.
Drag reduction measures such as micro-bubble injection and stepped hulls were considered. The conceptual utility of stepped hulls was discussed in connection with maximizing the favorable chines-dry flow regime on a planing surface. The top speed of the monohull concept design was shown to potentially increase from 52 knots to 58 knots for the same delivered power using a stepped hull.

The final monohull concept developed had a length overall of 81 feet and a beam of 17 feet. The top speed of the vessel was 52 knots and the cruise speed was 40 knots. The range for this craft at cruise speed was 650 nautical miles. The vessel was designed to operate continuously at 50 knots in sea state 3. The vessel was also designed to be air-transportable in a C17 cargo plane with no assembly or disassembly required.

The monohull concept exhibited minimal technical risk and can be considered a re-design of the current Mark V for air-transportation in a C17 cargo plane.

Trimaran: The design approach used for the trimaran concept was to modify the monohull design to incorporate two detachable side-hulls. The side-hulls were sized to allow air-transport of each hull in a C130 aircraft while the center-hull was transportable in a C17. The connection mechanism between the wing-hulls and center-hull allowed for assembly of the trimaran platform

at a remote forward insertion point. Further, the connection mechanism was designed to incorporate a quick disconnect feature to facilitate side-hull detachment allowing the side-hulls to perform manned or unmanned missions independent of the center-hull.

The side-hulls had an independent top speed of 82 knots having been designed with propulsion booster units that offer an increased speed capability compared to the single center-hull. The top speed of the trimaran concept was estimated to range from 56 to 61 knots. This represented a 4 to 9-knot increase in top speed compared with the monohull. The seakeeping performance was shown to markedly improve with the trimaran concept when compared with the monohull. Hence, when assembled, the trimaran high speed platform was designed to allow the SOF to travel faster and with less fatigue when compared with 80-foot class monohull designs.

The trimaran design also emphasized the integration of several vessels similar in characteristics to the current SOF fleet including, Mark V, HSAC, RHIB, CRRC, and PWC, into one common high speed platform.

The trimaran design displayed several attractive attributes. However, the trimaran concept was identified as posing significant technical risk. This risk was found to be most pronounced when the structure was considered to withstand the highly transient loads generated by this system when operating at high speed in a seaway. Structural dynamic FEA analyses were performed on models representing all major scantlings aft of the engine room bulkhead. These analyses indicated that additional structure, weighing in total 14,000 pounds, must be added to the conventional monohull design. This weight penalty represented nearly a 15% increase in the total weight of the monohull.

Conclusions

In summary, the monohull concepts could be implemented with traditional small craft naval architecture methods. Planing hulls with similar design attributes have a long history of successful operation. The design conclusions for the monohull include,

The trimaran concept offers several attractive attributes which are coupled to significant technical challenges that must be overcome for successful implementation of the design.

Characteristics of the trimaran design include,

- Modularity is used to integrate several vessels, similar to craft in the current SOF fleet, into one high speed platform;
- Option for manned and unmanned operation of side-hulls and other vessels are used in the concept;
- Increased seakeeping performance when compared to the monohull design;
- Increased top speed capability when compared to the monohull design;
- Significant challenges associated with designing structure to attach side-hulls to the centerhull;
- Detachment and reattachment of the wing structure from the centerhull to allow air-transportation provides additional operational and structural challenges;
- Detachment and reattachment of the side-hulls from wing structure introduces further operational and structural challenges; and,
- Operation in quartering seas will introduce additional maneuvering, seakeeping, and structural issues that must be addressed.

Acknowledgments

The authors would like to thank Battelle Memorial Institute, Raytheon, and the United States Special Operations Command for the opportunity to work on this interesting and challenging project.

The efforts and contributions of Ms. Constance Savander, Maritime Research Associates, L.L.C., are also gratefully acknowledged.

References

AKERS, R.H., HOECKLEY, S.A., PETERSON, R.S., AND TROESCH, A.W. (1999) Predicted vs. Measured Vertical-Plane Dynamics of a Planing Boat. FAST 1999. Seattle, Washington, USA.

AMERICAN BUREAU OF SHIPPING (2001) Guide for Building and Classing: High Speed Craft. Houston.

ALLEN, R.G. AND JONES, R.R. (1977) Considerations on the Structural Design of High Performance Marine Vehicles. SNAME, New York and Metropolitan Section Meeting, January 13.

BLOUNT, D.L. AND HANKLEY, D.W. (1976) Full Scale Trials and Analysis of High Performance Planing Craft Data. Transactions, SNAME, Vol. 84.

CLARK, V. (2002) SeaPower 21 Series Part I: Projecting decisive joint capabilities. Naval Institute Proceedings, October.

COOPER, S. AND NORTON, M. (2002) New paradigms in boat design: An exploration into unmanned surface vehicles. Association for Unmanned Vehicle Systems International Symposium.

FRIDSMA, G. (1971) A Systematic Study of Rough-Water Performance of Planing Hulls (Irregular Waves - Part II), Stevens Institute of Technology, March.

GALE, P.A. (2003) The Ship Design Process. Chapter 5, Ship Design and Construction. The Society of Naval Architects and Marine Engineers (SNAME), Jersey City, New Jersey, pp. 5-1 to 5-40.

HELLER, S.R. AND JASPER, N.H. (1960) On the Structural Design of Planing Craft. Quarterly Transactions, RINA. July.

HUGHES, O.F. (1988) Ship Structural Design: A Rationally-Based, Computer-Aided, Optimization Approach. SNAME, Jersey City.

SAVANDER, B.R. (1997) Planing Hull Steady Hydrodynamics. Ph.D. Thesis, Department of Naval Architecture and Marine Engineering, The University of Michigan.

SAVANDER, B.R., SCORPIO, S.M., AND TAYLOR, R.K. (2002) Steady Hydrodynamic Analysis of Planing Surfaces. SNAME, Journal of Ship Research, Vol. 46, No. 4.

SAVITSKY, D. AND BROWN, P.W. (1976) Procedures for Hydrodynamic Evaluation of Planing Hulls in Smooth and Rough Water. Marine Technology, SNAME, October 1976.

SOKOL, W. AND HANSEN, E. (2001) Unmanned vehicles: A technology whose time has come. July 2001 Excerpt. www.dt.navy.mil.

SPENCER, J.S. (1975) Sructural Design of Aluminum Crewboats. Marine Technology, SNAME, New York, July.

TULIN, M. P. (1957) The theory of slender planing surfaces at high speed. Schiffstechnik, 4, 1225-133.

VORUS, W.S. (1996) A flat cylinder impact theory for analysis of vessel impact loading and steady planing resistance. Journal of Ship Research, Vol. 40, No. 2, pp. 89-106.

WAGNER, H. (1932) Uber stross-und gleitvorgange an der oberflache von flussigkeiten. ZAMM, 12 pp. 193-215.

ZARNICK, E.E. (1978) A Nonlinear Mathematical Model of Motions of a Planing Boat in Regular Waves. David W. Taylor Naval Ship Research and Development Center. Report Number DTNSRDC-78/032.

ZARNICK, E.E. (1979) A Nonlinear Mathematical Model of Motions of a Planing Boat in Irregular Waves. David W. Taylor Naval Ship Research and Development Center. Report Number DTNSRDC/SPD-0867-01.